A Discrete Multiphase Approach For The Infiltration Of A Nanofluid Around A Staggered Microfiber Matrix

نظرية السريان المنفصل المتعدد الأطوار لانتشار سائل ممزوج بجزيئات صلبة ذات ابعاد بمقياس النانو حول مصفوفة غير منتظمة من الالياف ذات أبعاد بمقياس الميكرو

Ahmed Elgafy,
Associate Research Engineer,
University of Dayton Research Instuite, 300 College Park, Dayton, OH, 45469 USA

ملخص:

هذا البحث دراسة حسابية قائمة على نظرية السريان المنفصل المتعدد الأطوار(نظرية لاجرانج) و بهدف متابعة و استنباط مسارات الجزئيات ذات الابعاد بمقياس النانو والممزوجة في سائل خلال سريانه حول مصفوفة من الالياف غير منتظمة و ذات ابعاد بمقياس الميكرو. أظهرت النتائج التصاق بعض هذه الجزئيات على جدران الالياف مما قد يسبب انسداد المسارات داخل المصنوفة. لتلافى ذلك تم تفعيل دور الحمل القطعى المماسى (مارانجونى) مقترنا مع احداث فرق فى درجة الحرارة بين السائل و جدران الياف المصفوفة.

Abstract

In the present work a numerical study based on discrete multiphase approach, Lagrangian approach, is proposed to investigate and predict the trajectories of nanoparticles-filled fluid (nanofluid) infiltrated around a staggered microfiber matrix. The trajectory of the nanoparticle has been predicted by integrating the force balance on it in a Lagrangian reference frame during its motion through the fluid. The governing integral equations for the conservation of mass, momentum and energy have been solved in a segregated numerical fashion by a Control-Volume-Based Finite-Element Method. The nanoparticles trajectories and their interactions with fluid flow and microfiber walls have been predicted showing undesirable sticking tendency of the nanoparticles on the microfiber walls. To avoid this tendency, the contribution of Marangoni shear stress has been introduced coupled with a temperature difference between the fluid flow and the microfiber walls.

Keywords: Nanoparticles · Lagrangian approach · Trajectories · Solid/liquid interaction

1 Introduction

Nanoparticle flows have been emerging in numerous biological, and scientific applications, such as blood clogging and cell transport in arteries and veins, drug and gene delivery, and manufacturing of nanocomposites. Accordingly, many efforts are focused on the ability to create novel composites using nanocomposite materials as new matrices and to model various composite processes through numerical methods, Milton [1]; Kim et al. [2]; and Chen et al. [3]. In particular, enhancing and predicting the thermal performance of fluids and composites using of nanoparticle additives have been considered by many researchers Lee & Choi [4]; Xuan & Li [5];

Khanafer et al. [6]; Elgafy and Lafdi [7]. The presence of nanoparticles in fluids increases their effective thermal conductivities and consequently enhances their heat transfer characteristics Choi 1995 [8]; Lee et al. 1999 [9]; Xuan & Roetzel 2000 [10]; Eastman et al. 2001 [11]; Yu & Choi 2003 [12]. Besides thermal properties, nanoparticles additives may enhance mechanical properties of a given new system. In theory, carbon based nanoparticles could enhance both chemical and physical properties of composites Mauran et al. 1993 [13]; Py et al. 2001 [14]; Fukai et al. 2000 [15]. Moreover, fluids that contain nanoparticles additives (nanofluids) have a distinctive characteristic, which is quite different from those of traditional solid-

liquid mixtures in which millimeter and/or micrometer-sized particles are involved. Such particles could create pressure drop due to settling effects. In contrast, the nanofluids exhibit little or no penalty in pressure drop when flowing through the passages, Khanafer et al. [6]. Nevertheless, the possibility of clogging the micro-scale passages still exist due to interactions between the nanoparticle additives and the passage walls. This trend is magnified in case of some composite processes because of high resin viscosity and low preform permeability Conversely, and from fluid mechanics point of view, the flow of nanoparticle-filled fluids, nanofluids, is categorized as multiphase flow. Simulation and prediction of the characteristics of such flows could be very complex. Regardless of this complexity, significant progress has been made in different areas of multiphase Computational Fluid Dynamics, CFD. Wachem and Almsted [16] introduced different physical models for CFD predictions of multiphase flows while Kleinstreuer [17] introduced their numerical solution tools. It was depicted that there are two different basic approaches for studying this kind of flows. The first one is the continuum model, Eulerian approach, in which both the fluid phase and the solid phase are treated as continuous media, Jackson [18]. The second approach is the discrete particle model, Lagrangian approach, which treats the solid phase as separate particles that interact with the flow and traces the position and velocity of all the particles by solving Lagrangian equation of motion. The fluid phase is still considered as a continuum phase, and the effects of the solid phases are included by adding mass and force terms into the continuity and momentum equations of the fluid, Patankar and Joseph [19]. For both approaches, many other considerations should be taken in case of submicron and nano scales particles, Gidaspow [20]. As it is seen, Lagrangian

approach is appropriate for modeling multiphase problems that aim to study the behavior and interaction of the solid phase individuals, particles, with the continuous phase, fluid.

In the present paper, a two-dimensional simulation model based on Lagrangian multiphase approach for nanoparticle-filled fluid "nanofluid", which flows around staggered microfiber matrix, is introduced to investigate and predict the nanoparticles trajectories and their interactions with the fluid flow and the microfiber walls. Preventing any potential sticking of the nanoparticles on the microfiber walls is also a vital goal for the present study.

2 Numerical formulation
2.1 System configuration and physical domain
A nanofluid, which is composed of spherical carbon nanoparticles dispersed homogenously into a fluid, is infiltrated into a two-dimensional carbon microfiber matrix as shown in Fig. 1a. The microfibers have the same diameter D and are arranged in a staggered configuration with a separate distance T = D from all directions. The used nanofluid is assumed to be Newtonian, incompressible, laminar and its viscosity is not affected by small amount of nanoparticle additives. The infiltration process is supposed to occur during a short period (in second scale) while the second phase (nanoparticle) is sufficiently dilute that particle-particle interactions are negligible. A unit cell is taken as a representative unit cell for the system as shown in Fig. 1b, which illustrates that one-half of each side-by-side microfiber is only taken for symmetrical considerations, while the third microfiber, which is in a staggered orientation with the other two microfibers, is completely considered. As a case of study, carbon microfibers (8 μm in diameter) are considered, and a unit cell (16 μm x 38 μm)

represents the model. The carbon nanoparticles have a diameter of 100 nm. The thermo-physical properties of used fluid and solid particles (carbon nanoparticles) are listed in table 1.
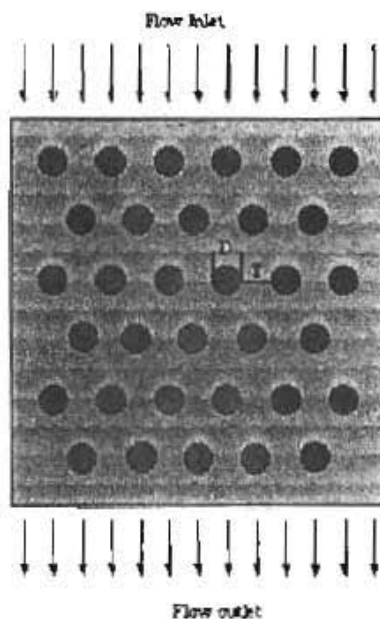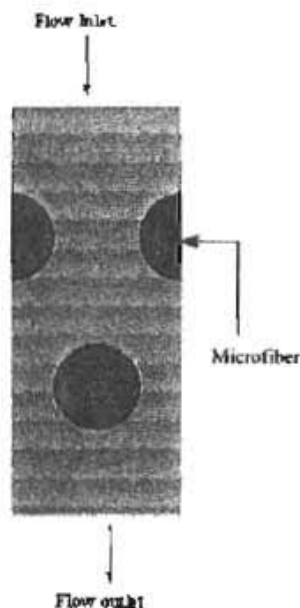

Fig. 1a Carbon microfibers matrix configuration

Fig. 1b Model's representative unit cell

Table 1: Thermophysical properties of the used fluid and solid nanoparticles

Property	
Density of fluid	1400 kg m^{-3}
Specific heat of fluid	1390 J kg^{-1} K^{-1}
Thermal conductivity of fluid	0.2 W m^{-1} K^{-1}
Viscosity of fluid	2.1 kg m^{-1} s^{-1}
Carbon nanoparticles density	2000 kg m^{-3}
Specific heat of solid nanoparticles	720 J kg^{-1} K^{-1}
Thermal conductivity of nanoparticles	200 W m^{-1} K^{-1}

2.2 Model description and governing equations

A two-dimensional simulation model based on Lagrangian multiphase approach for nanofluid, which is infiltrated around staggered microfiber matrix, is introduced to investigate and predict the nanoparticles trajectories and their interactions with the fluid flow and the microfiber walls. In this section, the governing equations of conservation of mass, momentum and energy of the system are introduced as well as the calculations of the nanoparticles trajectories coupling with the continuous phase, fluid.

2.2.1 Governing equations

In the present model, the fluid flow is considered as a two dimensional, steady laminar flow and the governing equations for conservation of mass, momentum and energy for two-dimensional axisymmetrical geometries, could be taken as follows:

2.2.1.1 Continuity equation

$$\frac{\partial \rho}{\partial t} + \frac{\partial}{\partial x}(\rho v_z) + \frac{\partial}{\partial r}(\rho v_r) + \frac{\rho v_r}{r} = S_m \quad .....(1)$$

where, x is the axial coordinate, r is the radial coordinate, ρ is the fluid density, v_x is the axial velocity, and v_r is the radial velocity and the source term S_m is the mass added to the continuous phase; resin, from the second phase; carbon nanoparticles.

2.2.1.2 Momentum equations

$$\frac{\partial}{\partial t}(\rho v_x) + \frac{1}{r}\frac{\partial}{\partial x}(r\rho v_x v_x) + \frac{1}{r}\frac{\partial}{\partial r}(r\rho v_r v_x) =$$

$$-\frac{\partial p}{\partial x} + \frac{1}{r}\frac{\partial}{\partial x}\left[r\mu\left(2\frac{\partial v_x}{\partial x} - \frac{2}{3}(\nabla \cdot \vec{v})\right)\right]$$

$$+\frac{1}{r}\frac{\partial}{\partial r}\left[r\mu\left(\frac{\partial v_x}{\partial r} + \frac{\partial v_r}{\partial x}\right)\right] + F_x \quad \dots\dots(2)$$

and

$$\frac{\partial}{\partial t}(\rho v_r) + \frac{1}{r}\frac{\partial}{\partial x}(r\rho v_x v_r) + \frac{1}{r}\frac{\partial}{\partial r}(r\rho v_r v_r) =$$

$$-\frac{\partial p}{\partial r} + \frac{1}{r}\frac{\partial}{\partial r}\left[r\mu\left(2\frac{\partial v_r}{\partial r} - \frac{2}{3}(\nabla \cdot \vec{v})\right)\right]$$

$$+\frac{1}{r}\frac{\partial}{\partial x}\left[r\mu\left(\frac{\partial v_r}{\partial x} + \frac{\partial v_x}{\partial r}\right)\right]$$

$$-2\mu\frac{v_r}{r^2} + \frac{2}{3}\frac{\mu}{r}(\nabla \cdot \vec{v}) + F_r \quad \dots\dots(3)$$

where p is the pressure, μ is the fluid viscosity, F is the external body forces that arise from interaction with the second phase, nanoparticles, and

$$\nabla \cdot \vec{v} = \frac{\partial v_x}{\partial x} + \frac{\partial v_r}{\partial r} + \frac{v_r}{r} \quad \dots\dots(4)$$

2.2.1.3 Energy equation

The energy equation for the present model is taken as given by Shin and Juree [21] in the following form

$$\frac{\partial(\rho cT)}{\partial t} + \nabla \cdot (\rho cT\vec{v}) = \nabla \cdot (k\nabla T) + S_h \quad \dots(5)$$

which, could be written as

$$\frac{\partial(\rho cT)}{\partial t} + \frac{\partial}{\partial x}(\rho cTv_x) + \frac{\partial}{\partial r}(\rho cTv_r) +$$

$$\rho cT\frac{v_r}{r} = \nabla \cdot (k\nabla T) + S_h \dots\dots\dots(6)$$

where, c and k are the fluid specific heat and thermal diffusivity respectively, T is the temperature and S_h is the heating source term.

2.3 Nanoparticles trajectory calculations
2.3.1. Equation of motion

The equation of motion for a representative particle in Lagrangian reference frame could be taken as given by Kleinstreuer [17] in the following form:

$$m_p\frac{d\vec{v}_p}{dt} = \vec{F}_{drag} + \vec{F}_{buoyancy} + \vec{F}_{pressure} +$$

$$\vec{F}_{virtualmass} + \vec{F}_{lift} + \vec{F}_{interaction} \quad \dots(7)$$

where, m_p and v_p are the particle mass and velocity respectively, and $d/dt = \partial/\partial t + \vec{v}_p \cdot \nabla$, i.e., a time derivative following the moving particle

2.3.2 Viscous drag force, $\vec{F}_{drag}$

The viscous drag force acting on the particle given by Kleinstreuer [17] is in the following form:

$$\vec{F}_{drag} = m_p C_d \frac{d(\vec{v}_f - \vec{v}_p)}{dt} \quad \dots(8)$$

where, $\vec{v}_f$ is the fluid velocity and C_d is the drag coefficient for submicron and nano scales particles given by Ounis et al. [22] and it has the form:

$$C_D = \left(\frac{18\mu}{C_c\rho_p d_p^2}\right) \quad \dots\dots(9)$$

where, μ is the fluid viscosity, ρ_p and d_p are the particle density and diameter respectively, and C_c is the Cunningham slip correction factor to Stokes' drag law, which can be computed from the following relation

$$C_c = 1 + \frac{2\lambda}{d_p}\left[1.257 + 0.4e^{-\left(1.1\frac{d_p}{2\lambda}\right)}\right] \dots(10)$$

where, λ is the molecular mean free path, Kleinstreuer [17].

2.3.4 Buoyancy force, $\vec{F}_{buoyancy}$

The net buoyant force acting on the particle is estimated from the following relation

$$\vec{F}_{buoyancy} = m_p(1 - \frac{\rho_f}{\rho_p})\vec{g} \dots\dots\dots(11)$$

where, ρ_f is the fluid density and g is the gravity.

2.3.5 Pressure force, $\bar{F}_{pressure}$

There pressure force acting on the particle is due to dynamic pressure and shear stress gradients, and its formula is given by Kleinstreuer [17] in the following form

$$\bar{F}_{pressure} = -V_p(\nabla p + \nabla . \bar{\bar{\tau}}) \quad \ldots \ldots (12)$$

where, V_p is the particle volume, p is the pressure and $\bar{\bar{\tau}}$ is the shear stress.

2.3.6 Virtual mass force, $\bar{F}_{virtualmass}$

The virtual mass force is the force required to accelerate the fluid surrounding the particle and it is taken as given by Kleinstreuer [17] in the form

$$F_{virtualmass} = \frac{1}{2}m_p \frac{\rho_f}{\rho_p} \frac{\hat{d}(\bar{v}_f - \bar{v}_p)}{\hat{d}t} \quad \ldots(13)$$

2.3.7 Lift force, $\bar{F}_{lift}$

The lift force due to shear, Saffman lift force, is taken as given by Li and Ahmadi [23] in the following form:

$$F_i^{lift} = 5.2m_p \frac{\rho_f v_f^{0.5} \varepsilon_{ij}(v_j^f - v_j^p)}{\rho_p d_p (\varepsilon_{lk}\varepsilon_{kl})^{1/4}} \quad \ldots(14)$$

where, v_f is the fluid kinematic viscosity and ε_{ij} is the deformation-rate tensor, which has the following form

$$\varepsilon_{ij} = \frac{1}{2}\left(\frac{\partial v_i}{\partial x_j} + \frac{\partial v_j}{\partial x_i}\right) \quad \ldots \ldots \ldots (15)$$

2.3.8 Interaction force, $\bar{F}_{interaction}$

In the present model we will consider the interaction forces due to Brownian motion effects. The Brownian force was modeled by Li and Ahmadi [24] as a Gaussian white noise random process where the amplitudes of the components at every time step, Δt:

$$F_i^{Brown} = G_i^{m_f}\left(\frac{\pi S_0}{\Delta t}\right) \quad \ldots \ldots (16)$$

where, G_i are the zero-mean, unit variance-independent Guassian random numbers; and S_0 is the spectral intensity;

$$S_n = 216 \frac{v_f \sigma T}{\pi^2 \rho_f d_p^5 \left(\frac{\rho_p}{\rho_f}\right)^2 C_c} \quad \ldots(17)$$

Where T is the absolute temperature of the fluid, σ is the Stefan – Boltzman constant, C_c is the Cunningham slip correction factor, equation (10).

2.4 Heat transfer calculations

To relate the particle temperature, $T_p(t)$, to the convective heat transfer a heat balance was performed and the following relation was utilized:

$$m_p c_p \frac{dT_p}{dt} = hA_p(T_f - T_p) \quad \ldots(18)$$

where: c_p and A_p are the heat capacity and the surface area of the particle, T_f is the local temperature of the continuous phase, fluid, h is the convective heat transfer coefficient.

As the particle trajectory is computed, equation (18) is integrated to obtain the particle temperature at the next time value, yielding:

$$T_p(t + \Delta t) = T_f + \left[T_p(t) - T_f\right]e^{-\beta_p \Delta t} \quad (19)$$

Where; Δt is the integration time step and

$$\beta_p = \left(\frac{A_p h}{m_p c_p}\right) \quad \ldots \ldots \ldots \ldots (20)$$

The heat transfer coefficient, h, is evaluated using the following correlation given by Incropera and DeWitt [25];

$$Nu = \frac{hd_p}{k_f} = 2.0 + 0.6 \, Re_d^{1/2} \, Pr_f^{1/3} \quad \ldots(21)$$

Where; k_f and Pr_f are is thermal conductivity and Prandtl number of the continuous phase, fluid, respectively and R_d is Reynolds number based on the particle diameter and the relative velocity.

2.5 Numerical solution

The numerical analysis has been performed using Fluent as follows. The momentum and heat exchanges from the continuous phase, fluid, to the discrete phase, nanoparticle, are computed by examining the change in momentum and thermal energy of the nanoparticle as it passes through each control volume in the model. These momentum and heat exchanges appear as momentum sink and source or sink energy in the continuous phase momentum and energy balances respectively in any subsequent calculations of the continuous flow field. During the motion of the particles, it is assumed that they do not exchange mass or heat by radiation with the continuous phase and they do not participate in any chemical reaction. The governing integral equations for the conservation of mass, momentum and energy for the model are solved in a segregated numerical fashion by a Control-Volume-Based Finite-Element Method, Patankar [26].

2.6 Grid size

A grid size of 50 x 120 is applied on the unit cell illustrated in Fig. 1b. To test and assess grid independence of the solution scheme, the grid size has been changed up to 50 x 120, and it has been found that this grid size is sufficient for the present case of study.

2.7 Initial and boundary conditions

The numerical model has been solved under the following assumptions and boundary and initial conditions: the thermophysical properties of the used fluid are introduced at a temperature level of $300^\circ K$. The flow inlet is defined by its velocity components, while the flow outlet is defined by its outlet pressure. The inlet velocity of the flow is assumed to be normal to the top boundary of the cell and has a magnitude of 0.05 m/s with the gravity direction and the flow outlet pressure is assumed to have the atmospheric

pressure value. Since the flow thermal solution is assumed to be periodic; periodic boundary conditions are applied on the side boundaries of the flow inlets and outlets. The carbon microfiber walls are assumed to have a temperature of $300^\circ K$ with no internal heat generation and no slip boundary condition. A condition of gravitational acceleration is also considered. Inert spherical carbon particles, which have a diameter of 100 nm, are injected through the fluid flow with different loads to investigate and predict the nanoparticles trajectories and their interactions with the fluid flow and the microfiber walls.

3. Results

The present model has been solved first for the flow of the sole fluid without the injection of the nanoparticles to study the flow characteristics and its interaction with the microfiber walls. As the main issue of the present study, the model has been solved with the injection of inert spherical carbon nanoparticles with fluid flow from different locations with different loads to investigate and predict nanoparticles trajectories and their interactions with the fluid flow and the microfiber walls.

3.1 Single fluid flow characteristics

The predicted static pressure contours for single fluid are illustrated in Fig. 2a. The figure shows that the maximum static pressure is achieved over the upper ends of the upper two microfibers due to their reactions against the fluid head. Also from this figure, one can see that the static pressure at the upper half of the cell decreases gradually towards the radial direction, r, and it has a minimum value at the cell center between the side-by-side microfibers. Conversely, the static pressure decreases sharply from the upper end to the lower end along the axial direction, x, until it

reaches a constant value at the lower half of the cell after passing the third microfiber.

The predicted dynamic pressure contours for single fluid are shown in Fig. 2b. Unlike the static pressure, the dynamic pressure increases from the wall sides toward the radial direction until it reaches maximum values at the center between the side-by-side microfibers. On the other hand, the dynamic pressure has less value around the third microfiber.

The predicted Reynolds number contours for the flow of single fluid are presented in Fig. 3a. The figure shows that the Reynolds number has minimum values around all microfiber walls as a result of high friction. The friction decreases gradually toward the center of the cell at the radial direction between the side-by-side microfibers where microfiber walls-fluid interaction diminished, while this friction decreases gradually around the third microfiber. Similarly, the shear stress is much higher at microfiber walls-fluid interface, Fig. 3b.
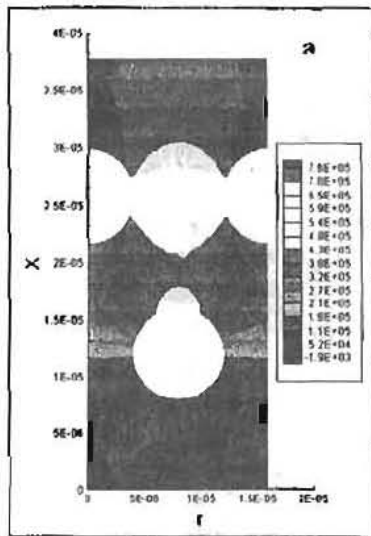
Fig. 2a Static pressure contours for single fluid in (Pa)
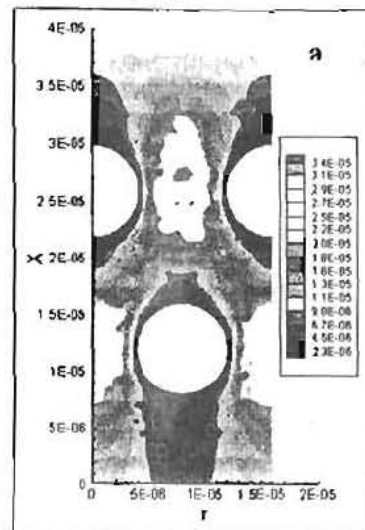
Fig. 3a Reynolds number contours for single fluid
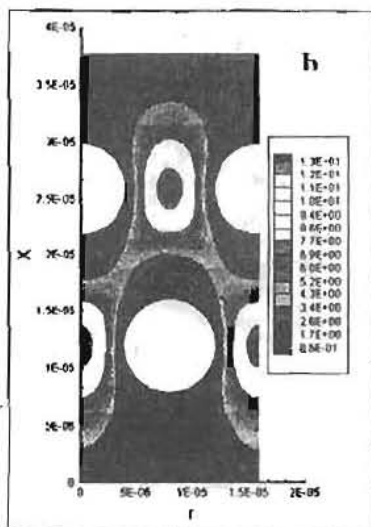
Fig.2b Dynamic pressure contours for single fluid in (Pa)
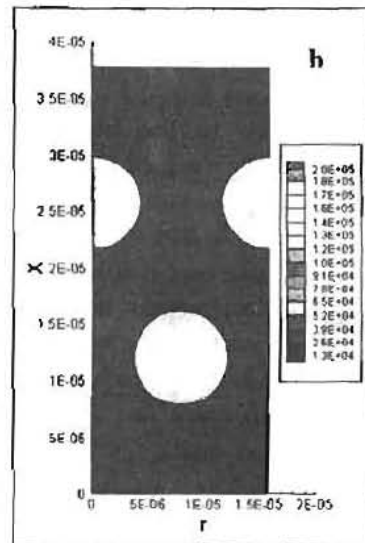
Fig.3b Walls shear stress contours for single fluid, (Pa).

3.2 Nanoparticles trajectories

The present model has been performed and solved for the injection of inert spherical carbon particles, which have a diameter of 100 nm, through the fluid flow from different locations of the system entrance with different nanoparticle load ratios. The nanoparticle trajectories for each case are predicted as well as their interactions with fluid flow and carbon microfiber walls.

3.2.1 Injection of nanoparticles with different load ratios

One nanoparticle has been injected through the fluid flow from the mid point of the unit cell entrance as shown in Fig. 4. The figure shows that the particle has moved directly between the two side-by-side microfibers until it has been trapped on the wall of the third microfiber. From this figure one can conclude that the effect of the two side-by-side microfibers on the nanoparticle motion has been eliminated by each other. Nevertheless, the particle could not survive when it has moved through the high friction zone around the third microfiber wall. On the other hand, when three nanoparticles have been injected between locations P(5e-06,3.7e-05) and P(1.55e-05,3.7e-05), which two of the particles are very close to the walls of the two side-by-side microfibers, all the particles have been trapped on the three microfiber walls due to the high friction effect, Fig. 5. The injection of nine nanoparticles between locations P(5e-06,3.7e-05) and P(1.55e-05,3.7e-05) is presented in Fig. 6. From the figure one can notice again that the nanoparticles, which have moved near the microfiber walls, have been trapped on their surfaces; while the other particles have the tendency to track the flow pattern around the microfibers walls.

The undesirable sticking tendency of the nanoparticles on the microfiber walls during the flow process, could occur because the interfacial fluid layers around the microfibers exhibit high friction. This friction tends to reduce the flow velocity, which may force some of the nanoparticles to stick on the microfiber walls and after sometime, perhaps, the flow passages will be blocked.
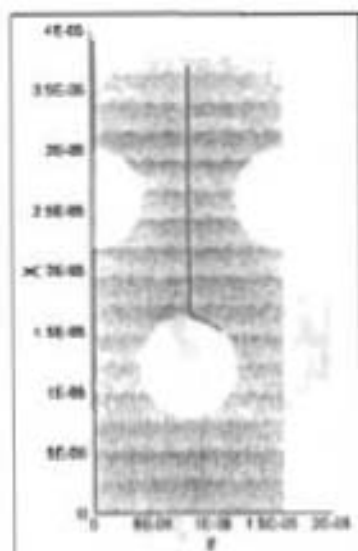

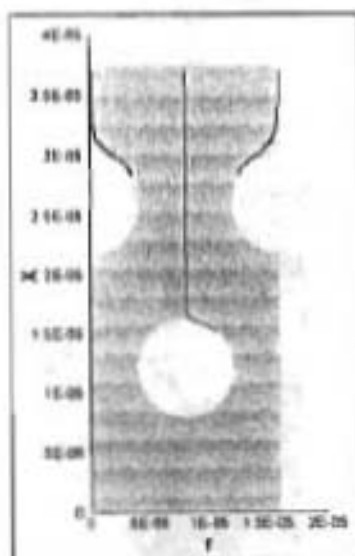Fig. 4 One particle injected from the mid point, P(8e-06, 3.7e-05)

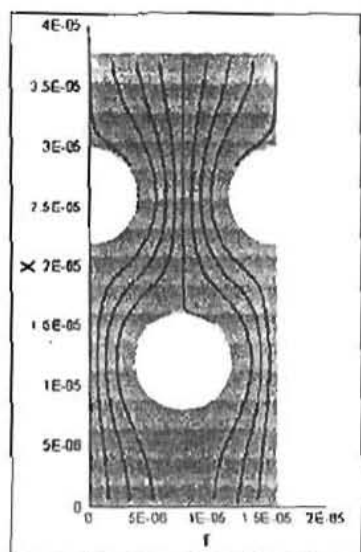Fig. 5 Three particles injected between two locations, P(5e-06,3.7e-05) and P(1.55e-05,3.7e-05)

Fig.6 Nine particles injected between two locations, P(5e-06,3.7e-05) and P(1.55e-05,3.7e-05

3.3. Contribution of Marangoni shear stress:

To prevent any potential sticking of the injected particles on the microfiber walls during the flow process; the contribution of Marangoni shear stress could be introduced coupled with a temperature difference between the fluid flow and the microfiber walls. As reported by Schwartz [27], the temperature-induced surface stress will contribute to the flow within the liquid layer. These thermocapillary effects give rise to various gravity independent phenomena including convective flows, interface distortions as well as interface rupture. Thermocapillary flows are driven by the imbalance of tangential stress on the interface caused by temperature dependence of surface tension, Jiang & Floryan [28]. This tangential stress is called Marangoni shear stress, and it has the following relation:

$$\tau_{Marangoni} = \frac{\partial \sigma}{\partial T} \cdot \frac{\partial T}{\partial s} \quad ...(22)$$

where $\dfrac{\partial \sigma}{\partial T}$ is the surface tension temperature coefficient and $\dfrac{\partial T}{\partial s}$ is the tangential vector of local free surface.

As it is seen from the definition of Marangoni shear stress, it is a combination between a surface tension and a temperature gradient, which offers a wealth of possible responses. To introduce the energy imbalance technique, the model has been performed and solved including the Marangoni shear stress contribution coupled with a temperature difference between the fluid flow and the microfiber walls. Many temperature difference levels have been applied while a fixed value of the surface tension temperature has been introduced, $\partial \sigma / \partial T = 0.4$ N/m.K.

The predicted temperature contours for various temperature difference levels for the sole flow are shown in Fig.7. As shown from the figure, temperature gradient has been built between the carbon microfibers walls and the fluid flow and this difference is getting stronger in the case of higher temperature difference levels.

The predicted Reynolds number contours for the sole flow after applying the new technique for different temperature levels are shown in Fig. 8. In general, one can see that introducing the new technique creates convective currents around the carbon microfiber walls, which cause kind of vortices around them. These vortices are forcing the flow to move away from the carbon microfiber walls and they are stronger in the case of higher temperature difference levels.
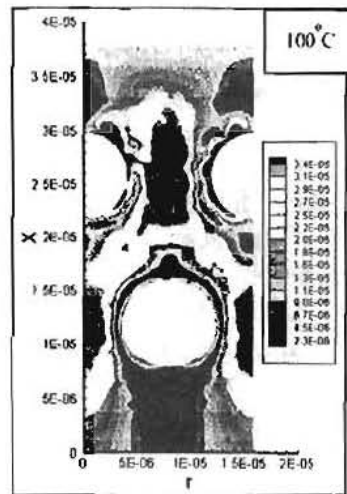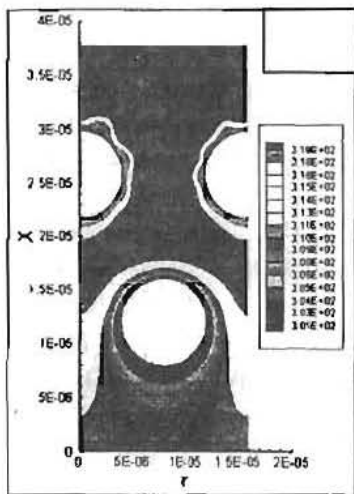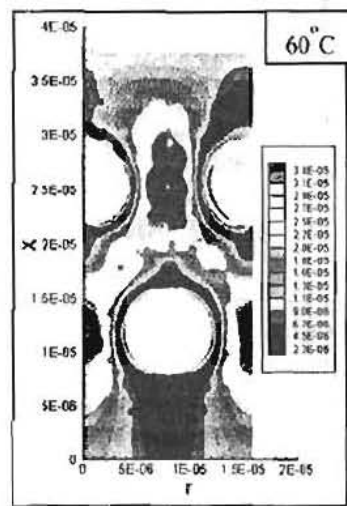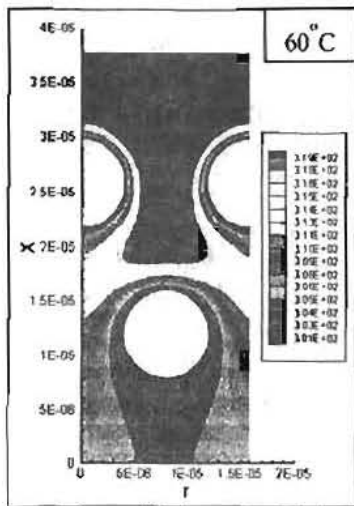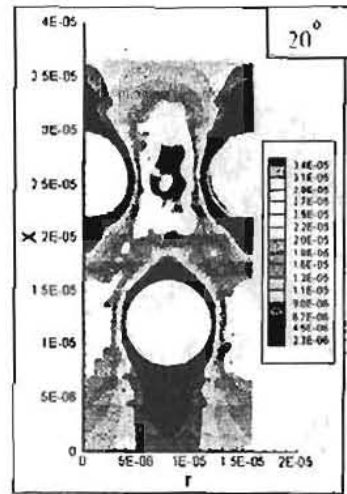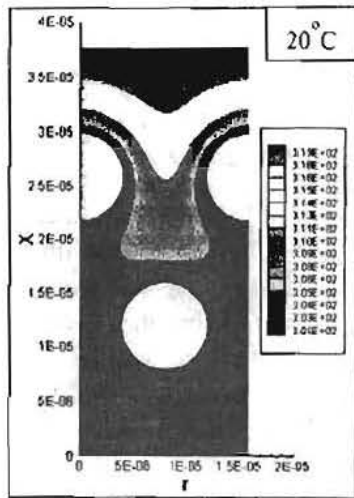
Fig. 7 Temperature contours for a temperature difference, ΔT, of 20, 60 and 100°C.

Figure. 8 Reynolds number contours for a temperature difference, ΔT, of 20, 60 and 100°C.

The predicted results for the trajectories of one and multiple nanoparticles after introducing the energy imbalance techniques are shown in Fig. 9 for a temperature difference level of 60 $^{\circ}$C. The figures show that the nanoparticles, which were trapped on the microfiber walls before introducing the technique, are moving away from the microfiber walls and they do not adhere on them.

4. Conclusions

A two-dimensional simulation model based on Lagrangian multiphase approach for nanoparticle-filled fluid "nanofluid" which flows around a staggered microfiber matrix, has been introduced. The nanoparticles trajectories and their interactions with fluid flow and microfiber walls have been investigated numerically showing undesirable sticking tendency of the nanoparticles on the microfiber walls. To prevent this tendency, the contribution of Marangoni shear stress has been introduced coupled with a temperature difference between the fluid flow and the microfiber walls. As a result of applying this technique, the nanoparticles, which had been trapped on the microfiber walls before introducing the technique, have moved away from the microfiber walls allowing the fluid to flow more smoothly around the microfiber walls, relative to its motion, before applying the energy imbalance technique.

The present numerical study tends to give an engineering solution to future composites processing using nanocomposite as new modified matrix to attend multifunctional properties.
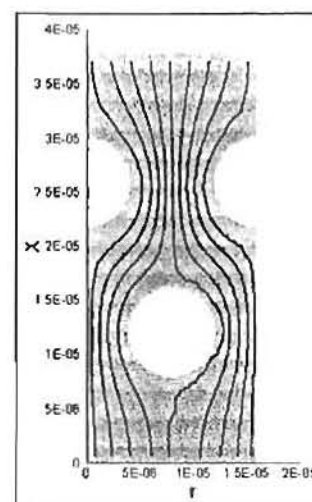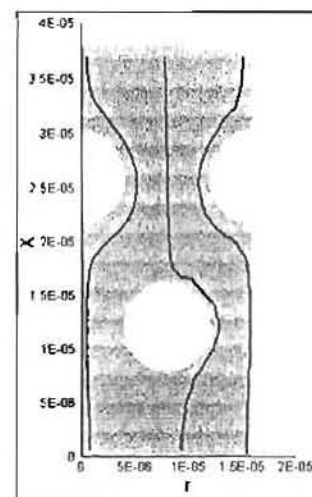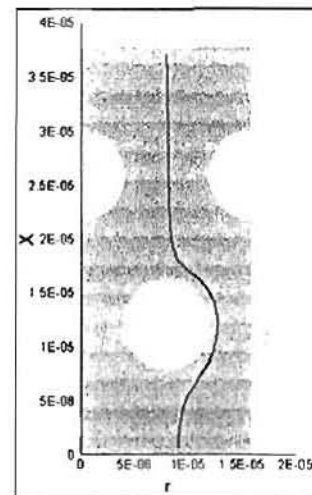

Fig. 9 Particles injection with different load ratios after introducing the energy imbalance technique

References

1- Milton G., "The theory of composites", Cambridge University Press, New York, 2002.

2- Kim K., Utracki A., and Kamal R., "Numerical simulation of polymer nanocomposites using self-consistent mean-field model", The Journal of Chemical Physics 121: 10766-10777, 2004.

3- Chen G., Tasciuc B., and Yang G., "In Encyclopedia of Nanoscience and Nanotechnology; edited by Nalwa H", American Scientific Publishers, Stevenson Ranch, California, vol. 7, N68, 2004.

4- Lee S., and Choi S., "Application of metallic nanoparticle suspensions in advanced cooling systems", ASME PVP 231: 227-234, 1996.

5- Xuan Y. and Li Q., "Heat transfer enhancement of nanofluids. Int. J. of Heat and Fluid Flow", 21: 58-64, 2000.

6- Khanafer K., Vafai K., and Lightstone M., "Buoyancy-driven heat transfer enhancement in a two-dimensional enclosure utilizing nanofluids", Int. J. of Heat and Mass Transfer 46: 3639-3653, 2003.

7- Elgafy A., and Lafdi K., "Effect of carbon nanofibers additives on thermal behavior of phase change materials", Carbon 43: 3067-3074, 2005.

8- Choi S. "Enhancing thermal conductivity of fluids with nanoparticles", ASME FED 231: 99-103, 1995.

9- Lee S., Choi S., Li S., and Eastman J., "Measuring thermal conductivity of fluids containing oxide nanoparticles", ASME J. Heat Transfer 121: 280-289, 1999.

10- Xuan Y., and Roetzel W., "Conceptions for heat transfer correlation of nanofluids", Int. J. of Heat and Mass Transfer 43: 3701-3707, 2000.

11- Eastman J., Choi S., Li S., Yu W., and Thompson L., "Anomalously increased effective thermal conductivities of ethylene glycol-based nanofluids containing copper nanoparticles", Applied Physics Letters 78: 718-720, 2001.

12- Yu W., and Choi S., "The role of interfacial layers in the enhanced thermal conductivity of nanofluids: A renovated Maxwell model", J. of Nanoparticle Research 5: 167-171, 2003.

13- Mauran S., Prades P., and L'haridon F., "Heat and mass transfer in consolidated reacting beds for thermochemical systems", Heat Recovery Systems & CHP 4: 315-319,1993.

14- Py X., Olives R., and Mauran S., "Paraffin/porous graphite-matrix composite as a high and constant power thermal storage material", Int. J. of Heat and Mass Transfer 44: 2727-2737, 2001.

15- Fukai J., Kanou M., Kodama Y., and Miyatake O., "Thermal conductivity enhancement of energy storage media using carbon fibers", Energy Conversion & Management 41:1543-1556, 2000.

16- Wachem B., and Almstedt A., "Methods for multiphase computational fluid dynamics", Chemical Engineering Journal 96: 81-98, 2003.

17- Kleinstreuer C., "Two-phase flow", Taylor & Frances, New York, 2003.

18- Jackson R., "Locally averaged equations of motion for a mixture of identical spherical particles and a Newtonian fluid", Chemical Engineering Science 52: 2457-2469, 1997.

19- Patankar A., and Joseph D., "Lagrangian numerical simulation of particulate flows", Int. J. of Multiphase Flow 27: 1685-1706, 2001.

20- Gidaspow D., "Multiphase flow and fluidization: continuum and kinetic theory descriptions", Academic Press, San Diego, California, 1994.

21- Shin S., and Juric D., "Modeling three-dimensional multiphase flow using a level contour reconstruction method for front tracking without connectivity", J. of Computational Physics 180: 427-470, 2002.

22- Ounis H., Ahmadi G., and McLaughlin B., "Brownian diffusion of submicrometer particles in the viscous sublayer", J. of Colloid and Interface Science 143: 266-277, 1991.

23- Li A., and Ahmadi G., "Computer simulation of particle deposition in the upper tracheobronchial tree", Aerosol Science and Technology 23: 202-223, 1995.

24- Li A., and Ahmadi G., "Dispersion and deposition of spherical particles from point sources in a turbulent channel flow", Aerosol Science and Technology 16: 209-226, 1992.

25- Incropera F., and DeWitt P., "Fundamentals of Heat and Mass Transfer", Fifth ed., Wiley, New York, 2002.

26- Patankar S., "Numerical heat transfer and fluid flow", Washington, DC: Hemisphere Publishing Corporation, 1980.

27- Schwartz L., "On the asymptotic analysis of surface-stress-driven thin-layer flow", J. of Engineering Mathematics 39:171-188, 2001.

28- Jiang Y., and Floryan J., "Effect of heat transfer at the interface on thermocapillary convection in adjacent phase", ASME J. Heat Transfer 125: 190-194, 2003.